World Conference on
Timber Engineering
Oslo 2023

RNN-BASED MONOTONIC LOADING BEHAVIOR PREDICTION OF CLT JOINTS

Yewei Ding[1],Haibei Xiong[2],Cheng Yuan[3],Lin Chen[4],Yurong Lu[5]

ABSTRACT: Cross-laminated timber (CLT) joints play an essential role in ensuring co-working performance between CLT structural parts and dissipating seismic energy when structures suffer earthquake. The variation of mechanical properties of CLT joints would further affect the whole structural safety. Thus, evaluating and predicting the loading behaviors of CLT joints is critical. In this research, the authors proposed a recurrent neural network (RNN)-based method to predict monotonic loading behaviors of CLT joints. Two RNNs models were adopted, including long short-term memory (LSTM) and gated recurrent unit (GRU). Further, the prediction performance of two RNNs models was compared using statistical and mechanical property index. Prediction results demonstrate that both LSTM and GRU models can predict the failure stage of the CLT joint with R^2 more than 0.90, λ_S and λ_T larger than 0.98. In the statistical index, the GRU model outperformed the LSTM model, although both models achieved the same accuracy in the mechanical property index. Overall, the RNN-based prediction method proposed in this study can provide an outstanding prediction performance for the monotonic mechanical behavior of CLT joints.

KEYWORDS: CLT joint, Mechanical properties, Monotonic loading, Recurrent neural networks (RNNs)

1 INTRODUCTION

Cross-laminated timber (CLT), as an engineering timber product, has recently become more popular in high-rise building construction due to its low carbon footprint and excellent mechanical properties[1]. For high-rise CLT constructions, joints play important roles in structural safety. Thus, it is significant to understand and predict mechanical properties of CLT joints.

To obtain loading behaviors of the CLT joint, many mechanical researches have been conducted. He et al. tested 3-layer and 5-layer CLT panels for bending, shear, and compressive strength. The research revealed the various failure modes of CLT bending and shear specimens, suggesting that the numerical model of the CLT bending specimens can predict initial elastic stiffness K_e and ultimate load-resisting capacity F_{max} [2]. Dong et al. taken research on the CLT shear wall anchored with tensile connections. The strength, stiffness, and ductility of sixty-eight groups of hold-down connections were investigated. The result demonstrated that the connections employed in their test could produce reasonably high ductility while avoiding the metal bracket fracture failures [3].

Mechanical tests can undoubtedly determine the loading behaviors of the CLT joint, but they are destructive and time-consuming. With the emerging improvement of artificial intelligence, machine learning algorithms have been utilized in predicting loading behaviors non-destructively and validated their feasibility. For example, Chen et al. evaluated and predicted damage degree of the bolt joint in glulam timber constructions via machine learning and received a high predicting accuracy of 96% [4]. When utilized for data-driven prediction, recurrent neural networks (RNNs) have the advantage of boosting efficiency and extracting damaged information from data as one of the machine learning algorithms [5]. In civil engineering, RNN models used to predict loading behaviors have made substantial progress. High accuracy prediction in hysteretic or constitutive behavior and nonlinear seismic response is made using RNN, such as long short-term memory (LSTM) and gated recurrent unit (GRU) [6]. However, no research towards predicting CLT joint loading behaviors has been published.

The purpose of this article is to predict the monotonic loading failure procedure of the CLT joint. Section 2 describes the mechanical tests of the CLT joint and explains the theory of the RNN models utilized in this paper. Section 3 displays the RNN model parameters and prediction result evaluation indexes. Section 4 and 5

[1] Yewei Ding, Tongji University, China, 2111383@tongji.edu.cn
[2] Haibei Xiong, Tongji University, China, xiong204@outlook.com
[3] Cheng Yuan, Tongji University, China, 20310146@tongji.edu.cn
[4] Lin Chen, Tongji University, China, 1710742@tongji.edu.cn
[5] Yurong Lu, Tongji University, China, 15250983931@163.com

https://doi.org/10.52202/069179-0154

contain the discussion and conclusion of the prediction results.

2 METHODOLOGY

Experiments were carried out in the methodology to determine the mechanical properties of the CLT joint and the materials. The tested values were then trained by two RNN models to predict the failure stage in the loading procedure. Finally, multiple indexes were used to evaluate the predicted load value. Figure 1 depicts the methodology's flowchart.

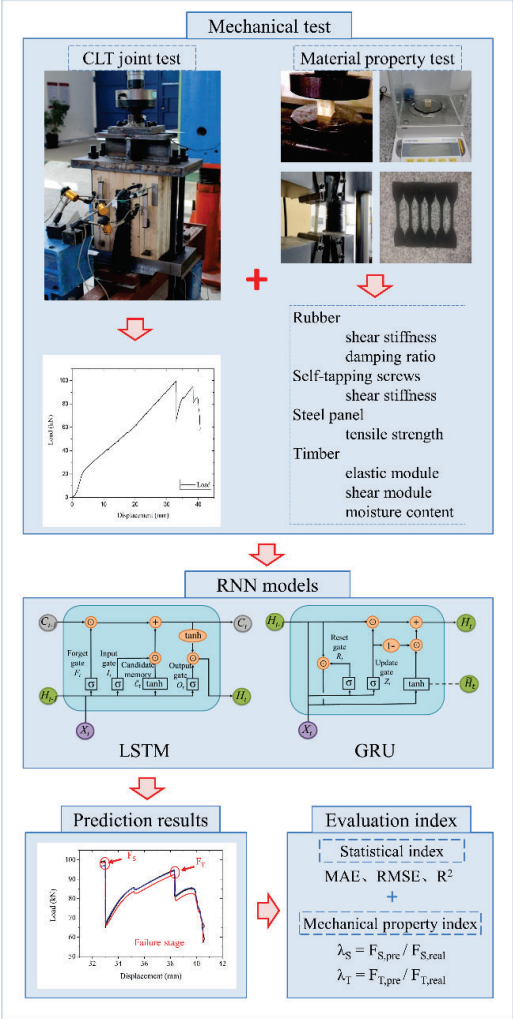

Figure 1: *Flowchart of the methodology*

2.1 MATERIALS AND PROPERTIES

The CLT panel was made with Canadian hemlock lumber and had a width of 300 mm and a height of 400 mm. Each panel was fabricated with 35/35/35 mm layups and a total thickness of 105 mm. According to the formal research, the connection used in this study employed energy-consuming rubber to reduce the interlayer displacement and improve the anti-seismic property, as shown in figure 2 [7]. The loading procedure in Hassanieh and Zhou's study included CLT joint failure with steel panel yielding, self-tapping screw cutting, and CLT panel broking [8,9]. So the mechanical properties of the steel panel, self-tapping screws, and CLT panels would influence the performance of the CLT joint. The mechanical properties of timber, self-tapping screws, and steel are tested according to the relevant standards and listed in table 1.

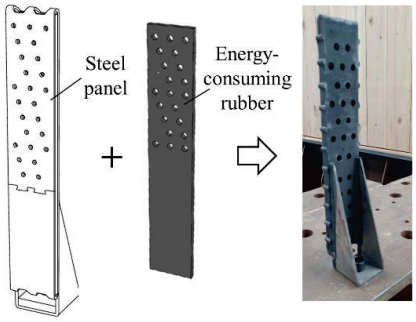

Figure 2: *Connection with energy-consuming rubber*

Table 1: *Value of material properties*

Material properties	Value
Shear stiffness of rubber	0.6 GPa
Damping ratio of rubber	0.2
Number of self-tapping screws	25
Shear stiffness of self-tapping screws	0.31 GPa
Tensile strength of steel	0.32 GPa
Elastic module of timber	15.31 GPa
Shear module of timber	1.17 GPa
Moisture content of timber	10.39%

2.2 TEST SETUP AND PROCEDURE

The monotonic loading approach used a two-stage displacement-control method (preloading procedure and formal loading procedure) according to ASTM D5652 [10]. The load was raised to 10% of the estimated peak load value during the preloading procedure, then unloaded after 2 minutes. In the formal loading procedure, the load was stopped when the joint reached the peak load or the displacement of 60 mm. Throughout the procedure, the loading speed is 1.5 mm/min. The CLT joint specimen and loading equipment are shown in figure 3.

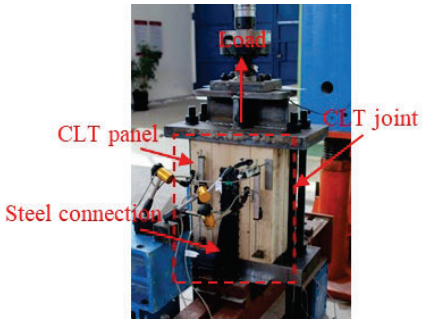

Figure 3: *CLT joint specimen and loading equipment*

2.3 TEST RESULTS

Figure 5 depicts the load-displacement curve of the monotonic loading procedure. The entire procedure, as

shown by the curve, is divided into three stages: elastic, plastic, and failure.

The wood fibers began to cut and crackle when the displacement reached 3 mm, and the joint entered the plastic stage. Following that, a part of the steel panel of the connection broke, causing the load suddenly decrease at the displacement of 33 mm, indicating that the procedure had entered the failure stage. The load was then supported by the energy-consuming rubber, the remaining steel panel, and the self-tapping screws. Finally, at the displacement of 38 mm, shear failure of the self-tapping screws resulted in the joint breaking and the load dropping precipitously.

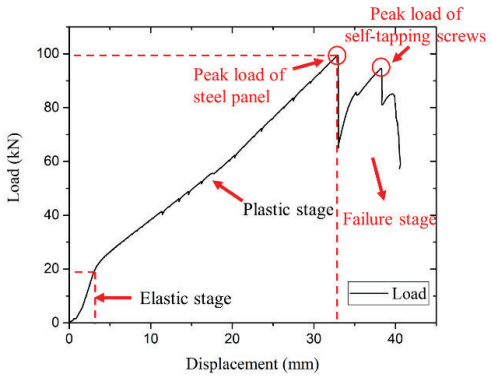

Figure 4: *Load-displacement curve*

2.4 RECURRENT NEURAL NETWORKS

Recurrent neural networks (RNNs) have been widely adopted as a kind of machine learning algorithm to predict sequential data [11]. One of the most widely used RNNs models is long short-term memory (LSTM). Long-term dependencies in the LSTM model are improved over traditional RNN models due to the gate functions introduced in the cell structure. Compared with the LSTM model, the gated recurrent unit (GRU) model has one fewer gate function, which may reduce the computational burden [12]. The LSTM model has been utilized to predict fracture growth rates of L-shape concrete specimens as well as the dynamic response of the nonlinear structure [13,14]. The GRU model has also been used in structural health monitoring (SHM) of civil structure buildings [15]. As a result, both the LSTM and the GRU models are effective methods for predicting loading behavior in civil engineering.

2.4.1 LSTM model

The LSTM model was initially introduced in 1997 and has received much attention in sequence prediction [16]. As shown in figure 3, variable weight matrixes are implemented by adding the input gate (I_t), forget gate (F_t), and output gate (O_t) in LSTM. Each gate includes a σ neural network layer and a pointwise multiply operation:

$$I_t = \sigma(X_t W_{xi} + H_{t-1} W_{hi} + b_i) \quad (1)$$

$$F_t = \sigma(X_t W_{xf} + H_{t-1} W_{hf} + b_f) \quad (2)$$

$$O_t = \sigma(X_t W_{xo} + H_{t-1} W_{ho} + b_o) \quad (3)$$

where X_t means input. H_{t-1} means the hidden state. σ is the activation function. W means the weight matrix, the first subscript of W refers to the input, and the second subscript refers to the gate. b means bias, and the subscript of b refers to the gate.

Candidate memory $\tilde{C}_t$ is expressed as:

$$\tilde{C}_t = tanh(X_t W_{xc} + H_{t-1} W_{hc} + b_c) \quad (4)$$

Memory cell C_t is expressed as:

$$C_t = F_t \odot C_{t-1} + I_t \odot \tilde{C}_t \quad (5)$$

Hidden state H_t is expressed as:

$$H_t = O_t \odot \tanh(C_t) \quad (6)$$

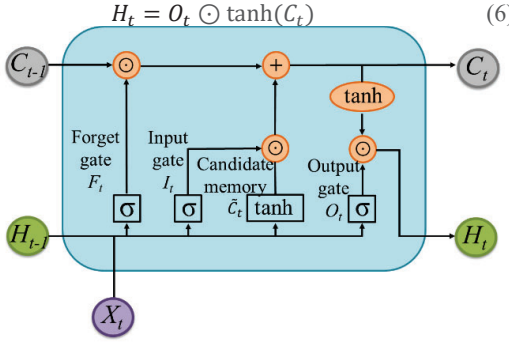

Figure 5: *Frame diagram of LSTM models*

2.4.2 GRU model

To decrease the computation burden, the LSTM model was improved into the GRU model with some cell states improved [17]. As shown in figure 6, the three gates in the LSTM model are integrated into the reset gate (R_t) and the update gate (Z_t) in the GRU model:

$$R_t = \sigma(X_t W_{xr} + H_{t-1} W_{hr} + b_r) \quad (7)$$

$$Z_t = \sigma(X_t W_{xz} + H_{t-1} W_{hz} + b_z) \quad (8)$$

where σ refers to the activation function, X_t means input, H_{t-1} means the hidden state, W represents the weight refers to different inputs and gates, b refers to bias.

The candidate hidden state $\widetilde{H}_t$ is expressed as:

$$\widetilde{H}_t = \tanh(X_t W_{xh} + (R_t \odot H_{t-1}) W_{hh} + b_h) \quad (9)$$

The hidden state H_t is expressed as:

$$H_t = Z_t \odot H_{t-1} + (1 - Z_t) \odot \widetilde{H}_t \quad (10)$$

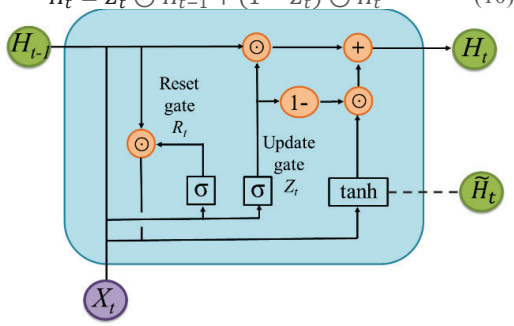

Figure 6: *Frame diagram of GRU models*

3 PREDICTION SETTINGS AND EVALUATION INDEX

3.1 PARAMETER SETTINGS

The load-displacement data obtained from the monotonic loading test are time-sequential. The mechanical testing

https://doi.org/10.52202/069179-0154

machine collected 300 data points per minute, fro a total of 8207 data points in the dataset. At that point, each data point contains the corresponding load, displacement, and material parameter. Although some parameters, such as the mechanical properties of CLT and steel, would change when entering the plastic stage, this study assumes that these material parameters would not change for simplification. In both LSTM and GRU models, the number of neurons is 8. The proportions of training and validation sets are 0.8 and 0.2, respectively.

In this research, rectified linear unit (ReLU) was adopted as the activation function to avoid the problem of disappearing gradients and to speed up training. Explained by equation (11) and figure 7:

$$f_x = \max(0, x) \tag{11}$$

where x is the output value from the previous layer.

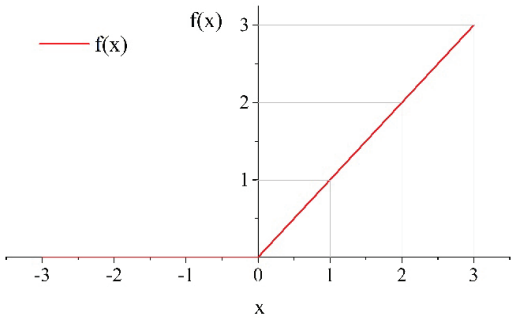

Figure 7: *Function image of ReLU*

Mean square error (MSE) is taken as the loss function in order to facilitate convergence:

$$MSE = \frac{\sum_{i=1}^{n}(y_i - x_i)^2}{n} \tag{12}$$

where x_i means real value, y_i means predicted value, n is the number of data.

Adaptive momentum is adopted to optimize. Furthermore, early stopping is employed for defending overfitting. Other parameter settings are listed in Table 2.

Table 2: *Parameter settings in RNN models*

Parameter	Value
Time step	40
Dropout	0.1
Epoch	100
Validation split	0.1
Batch size	32

3.2 EVALUATION INDEX

This paper presents two kinds of performance evaluation indexes (statistical and mechanical property indexes). Statistical indexes assess the fitness between predicted and real monotonic behavior obtained during the test. Mechanical property indexes are proposed as a mean of estimating predicted mechanical properties.

3.2.1 Statistical index

The statistical index contains mean absolute error (MAE), root mean square error (RMSE), and coefficient of determination (R^2). MAE and RMSE both indicate the error to the real value. Lower values of MAE and RMSE mean better prediction performance. The degree of fitness between predicted and real values is donated by R^2. When R^2 is close to 1.00, the prediction is more accurate. Three indexes are listed in equation (13-15):

$$MAE = \frac{\sum_{i=1}^{n}|y_i - x_i|}{n} \tag{13}$$

$$RMSE = \sqrt{\frac{\sum_{i=1}^{n}(y_i - x_i)^2}{n}} \tag{14}$$

$$R^2 = 1 - \frac{\sum_{i=1}^{n}(x_i - y_i)^2}{\sum_{i=1}^{n}(x_i - \bar{x})^2} \tag{15}$$

where x_i means real load value, $\bar{x}$ means mean real load value, y_i means predicted load value, n is the number of data in the load-displacement curve.

3.2.2 Mechanical property index

It is significant to evaluate the mechanical properties of the predicted results, which represent the loading behavior of the actual experiment. The broken steel panel and self-tapping screws of the CLT joint caused a sudden drop in load. As a result, the load value at these two points is adopted to evaluate the mechanical properties during the failure stage.

Based on the formal research [7], this study takes the coefficient of peak steel panel load λ_S as the normalized value of the predicted peak steel panel load based on the real value:

$$\lambda_S = F_{S,pre}/F_{S,real} \tag{16}$$

where $F_{S,pre}$ means the predicted peak steel panel load, the $F_{S,real}$ means the real peak steel panel load.

The coefficient of peak self-tapping screws load λ_T is similar to λ_S:

$$\lambda_T = F_{T,pre}/F_{T,real} \tag{17}$$

where $F_{T,pre}$ means the predicted peak self-tapping screws load, the $F_{T,real}$ means the real peak self-tapping screws load.

The closer λ_S and λ_T get to 1.00 representing a higher prediction accuracy.

4 RESULTS AND DISCUSSION

Figure 8 depicts the loading behaviors predicted by the LSTM and GRU models. Only the failure procedure is predicted. Load curves predicted by the LSTM and GRU models are both fit closely to the real load curve. Table 3 lists three statistical evaluation indexes. Both MAE and RMSE of the GRU model are lower than LSTM model's, while R^2 is higher, indicting that the GRU model's predicted results are statistically more precise than the LSTM model's.

https://doi.org/10.52202/069179-0154

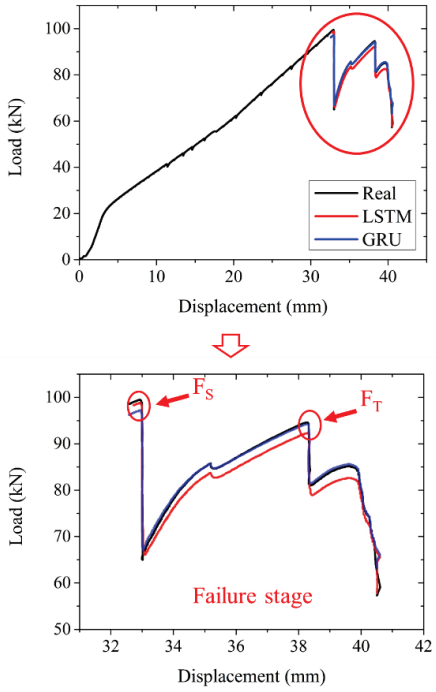

Figure 8: *Real and predicted load-displacement curve*

Table 3: *Statistical index*

Statistical index \ Model	LSTM	GRU
MAE (kN)	2.14	0.67
RMSE (kN)	2.58	1.62
R^2	0.91	0.97

Table 4 lists the peak loads predicted by the LSTM and GRU models for the steel panel and self-tapping screws, respectively. λ_S and λ_T are calculated according to the real and predicted load values. The λ_S and λ_T of the LSTM and GRU model are both higher than 0.98, which are close to 1.00. The LSTM model achieves λ_S of 0.99, which is higher than the 0.98 predicted by the GRU model. While the values of λ_T are the opposite. The high value of mechanical property indexes demonstrates the precise prediction ability of LSTM and GRU models.

Table 4: *Mechanical property index*

Mechanical property index \ Model	Real	LSTM	GRU
F_S (kN)	99.50	98.80	97.20
F_T (kN)	94.61	92.30	94.20
λ_S	--	0.99	0.98
λ_T	--	0.98	1.00

As stated in section 2.4, the GRU model has a lower computational burden than the LSTM model. The LSTM model consumed 14 seconds and 92 milliseconds in this study, while the GRU model took 14 seconds and 54 milliseconds. Given that the number of predicted data points in this monotonic loading test is 1641, the GRU model consums only 38 milliseconds less than the LSTM model. In case of tests containing a large amount of data points, such as hysteretic loading tests or other complex and time-consuming tests, the computation reduction and time-saving effect of the GRU model will be more obvious.

5 CONCLUSIONS AND PROSPECT

The authors proposed an RNNs-based prediction method for the failure procedure of CLT joint under monotonic loading in this paper. Statistical indexes (MAE, RMSE, and R^2) and mechanical property indexes (λ_S and λ_F) are used to evaluate the predicted load-displacement curves.. The MAE of the LSTM and GRU model are both no higher than 2.14 kN, while the RMSE of the two RNN models is no higher than 2.58 kN, and R^2 is greater than 0.91. The values of the three statistical indexes indicated that the error between the predicted value and real value is small. Furthermore, both λ_S and λ_T of the LSTM and GRU model are greater than 0.98, indicating that the two models predict the peak load of the steel panel and self-tapping screws of the joint with a high accuracy . The high value of the prediction indexes demonstrates that both the LSTM and GRU models accurately predicted the failure procedure of CLT joint under monotonic loading precisely, with the GRU model outperforming the LSTM model in terms of statistical indexes.

Prediction accuracy demonstrated the feasibility and effectiveness of using the RNN-based method to predict the failure procedure of CLT joints, providing a reference for CLT construction mechanical properties research.

The mechanical properties of the materials in the RNN model, on the other hand, remained constant throughout the loading procedure, whereas the stress varies with strain during the actual loading procedure. Therefore, in the future work, the constitutive model of the materials would be considered for more accurate physics expression and prediction results.

ACKNOWLEDGEMENT

The authors are thankful for the support of the National Natural Science Foundation of China (51978502).

REFERENCE

[1] Brandner R., Flatscher G. and Ringhofer A. et al. Cross laminated timber (CLT): overview and development. *Eur J Wood Wood Prod*, 74(3): 331-351, 2016.

[2] He M., Sun X. and Li Z. et al. Bending, shear, and compressive properties of three- and five-layer cross-laminated timber fabricated with black spruce. *J Wood Sci*, 66(1), 2020.

[3] Dong W., Li M. and Ottenhaus L. et al. Ductility and overstrength of nailed CLT hold-down connections. *Eng Struct*, 215: 110667, 2020.

https://doi.org/10.52202/069179-0154

[4] Chen L., Xiong H. and Yang Z. et al. Preload measurement of steel-to-timber bolted joint using piezoceramic-based electromechanical impedance method. *Measurement*, 190: 110725, 2022.
[5] Shajihan S. A. V., Wang S. and Zhai G. et al. CNN based data anomaly detection using multi-channel imagery for structural health monitoring. *Smart Struct Syst*, 29(1): 181-193, 2022.
[6] Sajjad M., Khan Z. A. and Ullah A. et al. A Novel CNN-GRU-Based Hybrid Approach for Short-Term Residential Load Forecasting. *Ieee Access*, 8: 143759-143768, 2020.
[7] Chen J., Xiong H. and Furuta T. et al. Experimental and analytical studies on mechanical performance of innovative energy-dissipating hold-down for CLT structures. *Constr Build Mater*, 317: 125966, 2022.
[8] Zhou Q., Gong M. and Chui Y. H. et al. Measurement of rolling shear modulus and strength of cross laminated timber fabricated with black spruce. *Constr Build Mater*, 64: 379-386, 2014.
[9] Hassanieh A., Valipour H. R. and Bradford M. A. Composite connections between CLT slab and steel beam: Experiments and empirical models. *J Constr Steel Res*, 138: 823-836, 2017.
[10] ASTM D5652-21. Standard Test Methods for Single-Bolt Connections in Wood and Wood-Based Products. *ASTM International*, United States, 2021.
[11] Yu Y., Si X. and Hu C. et al. A Review of Recurrent Neural Networks: LSTM Cells and Network Architectures. *Neural Comput*, 7(31): 1235-1270, 2019.
[12] Cho K., van Merrienboer B. and Bahdanau D. et al. On the Properties of Neural Machine Translation: Encoder‐Decoder Approaches. *Statistics-Abingdon*, 2, 2014.
[13] Xue J. and Ou G. Predicting wind-induced structural response with LSTM in transmission tower-line system. *Smart Struct Syst*, 3(28): 391-405, 2021.
[14] Le Hien Nguyen D., Thi Thanh Do D. and Lee J. et al. Forecasting Damage Mechanics by Deep Learning. *Computers, Materials & Continua*, 61(3): 951-977, 2019.
[15] Liu Y. WSN-Based SHM Optimisation Algorithm for Civil Engineering Structures. *Processes*, 10(10): 2113, 2022.
[16] Hochreiter S. and Schmidhuber J. Long Short-Term Memory. *Neural Comput*, 1997.
[17] Dey R. and Salem F. M. Gate-Variants of Gated Recurrent Unit (GRU) Neural Networks. *Statistics-Abingdon*, 2017.